APPLIED AND ENVIRONMENTAL MICROBIOLOGY, Oct. 2002, p. 4731–4739 Vol. 68, No. 10
0099-2240/02/$04.00+0 DOI: 10.1128/AEM.68.10.4731–4739.2002

Engineering of Primary Carbon Metabolism for Improved Antibiotic Production in *Streptomyces lividans*†

Michael J. Butler,[1]* Per Bruheim,[2] Srdjan Jovetic,[3] Flavia Marinelli,[3] Pieter W. Postma,[4]‡ and Mervyn J. Bibb[1]§

Department of Molecular Microbiology, John Innes Centre, Norwich, NR4 7UH, United Kingdom[1]; Department of Biotechnology, Norwegian University of Science and Technology, N7491 Trondheim, Norway[2]; Biosearch Italia S.p.A., 21040 Gerenzano (VA), Italy[3]; and E. C. Slater Institute, Faculty of Chemistry, University of Amsterdam, 1018WS Amsterdam, The Netherlands[4]

Received 29 March 2002/Accepted 11 July 2002

Deletions were made in *Streptomyces lividans* in either of two genes (*zwf1* and *zwf2*) encoding isozymes of glucose-6-phosphate dehydrogenase, the first enzyme in the oxidative pentose phosphate pathway (PPP). Each mutation reduced the level of Zwf activity to approximately one-half that observed in the wild-type strain. When the mutants were transformed with multicopy plasmids carrying the pathway-specific transcriptional activator genes for either the actinorhodin (ACT) or undecylprodigiosin (RED) biosynthetic pathway, they produced higher levels of antibiotic than the corresponding wild-type control strains. The presumed lower flux of carbon through the PPP in each of the Δ*zwf* mutants may allow more efficient glucose utilization via glycolysis, resulting in higher levels of antibiotic production. This appears to occur without lowering the concentration of NADPH (the major biochemical product of the oxidative PPP activity) to a level that would limit antibiotic biosynthesis. Consistent with this hypothesis, deletion of the gene (*devB*) encoding the enzyme that catalyzes the next step in the oxidative PPP (6-phosphogluconolactonase) also resulted in increased antibiotic production. However, deletion of both *zwf* genes from the *devB* mutant resulted in reduced levels of ACT and RED production, suggesting that some of the NADPH made by the PPP is utilized, directly or indirectly, for antibiotic biosynthesis. Although applied here to the model antibiotics ACT and RED, such mutations may prove to be useful for improving the yield of commercially important secondary metabolites.

The emergence of multiply antibiotic-resistant human pathogens has resulted in an urgent need for new antibiotics. Actinomycetes produce approximately two-thirds of all known antibiotics of microbial origin, including over 6,000 different chemical structures, and they continue to be an excellent source of novel compounds. Many of these natural products are commercially important medicinal compounds with a variety of therapeutic uses. Frequently, antibiotics are grouped on the basis of common or similar biosynthetic pathways (e.g., members of the polyketide, polyether, macrolide, and β-lactam families), and they are often produced from the same primary metabolic precursors.

One of the hurdles in the development of a newly discovered natural product as an antibiotic or in the development of a novel antibiotic made by combinatorial biosynthesis (16) is the ability to generate sufficient quantities of the compound for further study. Genetic manipulation of a producing organism can be used to improve the efficiency of production, which is classically achieved by empirical means but more recently has been conducted in a knowledge-based manner (8). One potentially important element in productivity is the availability of precursors and cofactors.

We chose to study *Streptomyces lividans* 66 strains containing multicopy plasmids carrying the pathway-specific transcriptional activator gene for either actinorhodin (ACT) (pIJ68) (30) or undecylprodigiosin (RED) (pIJ6014) (38). These strains each produced copious amounts of only one antibiotic (either ACT or RED), and they were presumed to contain such high levels of the pathway-specific activators that the antibiotic biosynthetic enzymes should not limit metabolic flux. Rather, it was assumed that the supply of metabolic precursors for antibiotic biosynthesis was limiting and might be manipulated to improve the antibiotic production capability.

Most antibiotic biosynthetic pathways involve some reductive steps in which NADPH is used as an essential cofactor. In most cells the majority of NADPH is produced by the activity of two enzymes of the pentose phosphate pathway (PPP), glucose-6-phosphate dehydrogenase (G6PDH) (Zwf) and 6-phosphogluconate dehydrogenase (6PGDH) (36). However, in *S. lividans* 6PGDH was reported to use NAD^+ in preference to $NADP^+$ as a cofactor (12). In *Streptomyces antibioticus*, glucose is catabolized by both the PPP and glycolysis, and the PPP is the dominant pathway during exponential growth (34). Of particular relevance to these studies is the fact that a positive correlation was observed between methylenomycin production and carbon flux through the PPP in *Streptomyces coelicolor* (26). This suggested that it might be possible to enhance antibiotic production by increasing the supply of NADPH by elevating the activity of Zwf. To address this possibility, deletions were made in the *zwf* genes of *S. lividans* in order to

* Corresponding author. Mailing address: Department of Molecular Microbiology, John Innes Centre, Colney Lane, Norwich, NR4 7UH, United Kingdom. Phone: (44) 1603450000. Fax: (44) 1603450778. E-mail: michael.butler@bbsrc.ac.uk.

† This paper is dedicated to the memory of Pieter Postma for his immense contribution to the field of bacterial physiology. He was a true friend and colleague who will be missed enormously.

‡ Deceased.

§ Present address: Diversa Corporation, San Diego, CA 92121.

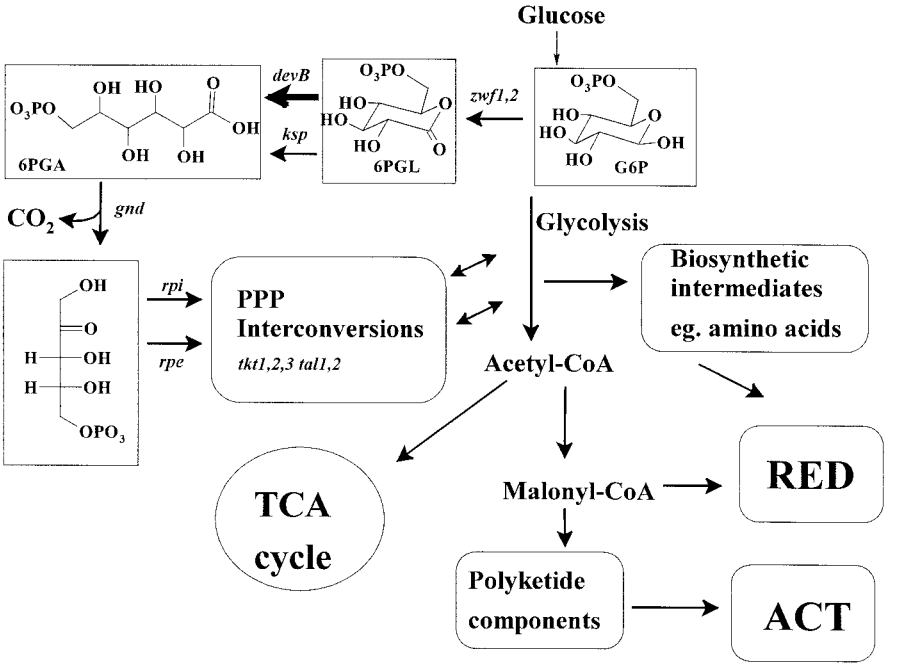

FIG. 1. Overview of central carbon metabolism, showing the early steps of the PPP. Genes encoding the enzymes relevant to this work are shown. 6PGA, 6-phosphogluconate; *ksp*, spontaneous hydrolysis of 6-phospho-δ-gluconolactone (6PGL); G6P, glucose-6-phosphate; TCA, tricarboxylic acid; CoA, coenzyme A.

assess the contribution of the PPP to ACT and RED biosynthesis in derivatives of a strain that had been engineered to overproduce each of the antibiotics. Once the expected reduction in antibiotic biosynthesis had been observed in the *zwf* mutants, elevated levels of NADPH could then be engineered by overexpression of the appropriate genes, with the expectation that this would result in enhanced antibiotic production. *S. coelicolor* is closely related to *S. lividans*, and some primary metabolic genes show high levels of nucleotide sequence identity (e.g., *glkA*, encoding glucose kinase, shows 99.8% identity over 904 nucleotides [22]). Two clusters of genes encoding PPP enzymes were identified during the *S. coelicolor* genome sequencing project (http://www.sanger.ac.uk/Projects/*S_coelicolor*/; accession numbers AL031107 and AL096839). The genes appear to be organized into operons with many of the predicted translational initiation and termination sites either overlapping or lying extremely close together, suggesting that many of the genes are translationally coupled. Both clusters contain genes for transketolase (*tkt*) and transaldolase (*tal*) that lie 5′ of the *zwf* genes. The *zwf* genes (*zwf1* and *zwf2*) of each cluster appear to be translationally coupled with downstream *opc* genes that are essential for Zwf activity in both cyanobacteria (14, 37) and *Corynebacterium glutamicum* (25). The deduced amino acid sequences of Zwf1 and Zwf2 from *S. coelicolor* are very similar (85% identity), whereas the two Zwf proteins in *Mycobacterium tuberculosis* (10) show only 50% identity to each other. Both *S. coelicolor* Zwf proteins are markedly more similar to *M. tuberculosis* Zwf2 (75 and 77% identity for *zwf1* and *zwf2*, respectively) than to Zwf1 (51 and 49% identity, respectively). The product of *devB*, which lies immediately downstream of *opc* in the *zwf2* gene cluster, shows homology to an additional N-terminal domain found in a mammalian G6PDH. This domain is not directly involved in G6PDH catalytic activity but has recently been shown to encode the 6-phosphogluconolactonase (15). This enzyme catalyzes hydrolysis of the lactone (which undergoes slow spontaneous hydrolysis in the absence of the lactonase) to produce the substrate for the 6PGDH (Fig. 1).

MATERIALS AND METHODS

Bacterial strains, media, and plasmids. *Escherichia coli* strains DH5α (35) and ET12567 (21) were used for routine subcloning and conjugation into *S. lividans*, respectively. Organisms were grown at 37°C in Luria-Bertani medium, and for transformation we used standard procedures (35). *E. coli* transformants were selected with carbenicillin (100 $\mu g \cdot ml^{-1}$), apramycin (50 $\mu g \cdot ml^{-1}$), or hygromycin (50 $\mu g \cdot ml^{-1}$). The cloning vectors used were pIJ2925, pIJ2920 (18), pKC1132 (3), and pGEM-T (Promega). *S. lividans* 66 (John Innes Centre strain 1326) and *S. coelicolor* M145 were grown and manipulated as described previously (18). For conjugation from *E. coli* we used helper plasmid pUZ8002 (27). *S. lividans* exconjugants were selected by adding 0.5 mg of nalidixic acid and 1 mg of apramycin or 1 mg of hygromycin to each agar plate. Strains were purified and maintained by using 20 μg of apramycin per ml or 20 μg of hygromycin per ml.

For shake flask fermentation experiments we used a 50-ml seed stage culture containing a mixture of 2 parts of yeast extract-malt extract medium and 1 part of Trypticase soy broth containing thiostrepton at a concentration of 50 $\mu g \cdot ml^{-1}$. Spores were inoculated directly into 250-ml conical spring flasks containing this medium and were incubated with shaking at 30°C for 40 to 44 h. Mycelium was collected by centrifugation and resuspended in a liquid minimal medium (6) containing 25 g of glucose per liter and 25 μg of thiostrepton per ml. The cultures were fermented for up to 7 days and monitored daily until antibiotic accumulation ceased.

For stirred-tank fermentation experiments, strains were stored as frozen mycelium at −80°C. The stock cultures were used to inoculate (1%, vol/vol) 100-ml portions of GG1 medium (15 g of glucose per liter, 15 g of glycerol per liter, 15 g of soy peptone per liter, 3 g of NaCl per liter, l g of $CaCO_3$ per liter, 0.005 g of thiostrepton per liter) in 500-ml baffled Erlenmeyer flasks. Cultures were grown for 48 h at 28°C on a rotary shaker at 200 rpm. Then 8 ml of each culture was used to inoculate 100 ml of GYB medium (33 g of glucose per liter, 15 g of yeast extract per liter, 0.005 g of thiostrepton per liter) in a 500-ml baffled flask. The cultures were grown for 24 h at 28°C on a rotary shaker at 200 rpm, and 100-ml

TABLE 1. *S. lividans* mutant strains used in this work

Strain	Genotype	Deletion plasmid	Brief description of deletion
M704	Δ*zwf1*	pIJ8702	In-frame deletion in *zwf1*
M706	Δ*zwf1* Δ*zwf2-opc2-devB*	pIJ8706	In-frame deletion in *zwf1*; deletion of majority of *zwf2* and all of *opc2* and *devB* at the 3′ end of *zwf2* transcription unit
M714	Δ*devB*	pIJ8718	Deletion of *devB* at the 3′ end of *zwf2* transcription unit; hygromycin resistance gene inserted in place of *devB*
M715	Δ*zwf2*	pIJ8717	In-frame deletion in *zwf2*

portions were used to inoculate 4-liter fermentors containing 2.5 liters of phosphate-limited Evans medium.

PCR conditions. Appropriate oligonucleotide primers were used with the ExpandHF PCR system (Boehringer). After an initial denaturation step (3 min at 96°C), 20 cycles of amplification (1 min at 94°C, 1 min at 50°C, 1 min per kb of DNA at 68°C) was followed by a final extension period of 15 min at 72°C. *Taq* polymerase (Boehringer) was used for other PCRs when the presence or absence of a particular fragment needed to be determined.

Construction of plasmids and mutant strains. The mutant strains made in this work are listed in Table 1.

(i) *S. lividans* M704 (Δ*zwf1*). To make an in-frame deletion in *zwf1*, a DNA fragment that contained the 3′ end of *zwf1* and flanking DNA (length, 1.7 kb) was first produced by PCR. Cosmid SC5A7 was used as the DNA template with primers g6pdh1 and g6pdh2 (Table 2), and the amplified fragment was cloned into pGEM-T, which introduced a *Hin*dIII site downstream of the 3′ end of the *zwf1* sequence. The resulting plasmid was designated pIJ8719. The nucleotide sequences of the ends of the cloned DNA were confirmed by using universal and reverse primers. The internal sequence of the DNA was confirmed by using sequencing primers g6pdh.seq1 to g6pdh.seq4. A second DNA fragment containing the 5′ end of *zwf1* and flanking DNA was purified as a 2.8-kb *Bam*HI fragment from the same cosmid and cloned into the *Bam*HI site of pIJ2925, yielding pIJ8720. Insertion of the 1.7-kb *Hin*dIII-*Mlu*I fragment from pIJ8719 into pIJ8720 that had been digested with the same enzymes led to replacement of the 3′ end of *zwf1*, generating the required in-frame deletion. The overall result was deletion of a 1,113-bp *Mlu*I fragment (within the *zwf1* coding region) which was now flanked by 1.7- and 1.8-kb DNA fragments. This fragment was excised by using *Hin*dIII and *Eco*RI sites flanking the *Bam*HI site in pIJ2925 and cloned between the *Hin*dIII and *Eco*RI sites of pKC1132 (which carries an apramycin resistance gene) to produce pIJ8722. The desired deletion was confirmed by nucleotide sequencing, and the plasmid was introduced into *S. lividans* 1326 by conjugation. Apramycin-resistant exconjugants were grown nonselectively to allow excision of the integrated DNA. Apramycin-sensitive colonies were examined by Southern hybridization to assess whether they segregated to yield the wild-type or *zwf1*-deleted genotype. When the labeled 2.8-kb *Bam*HI DNA fragment (Fig. 2a) was used to probe *Bam*HI-digested chromosomal DNAs, the wild-type DNA showed a strong signal at 2.8 kb, whereas the two mutant DNA samples produced the larger band expected for deletion of the *Mlu*I fragment, which contained a *Bam*HI site. These *zwf1* mutant strains were designated M704-1 and M704-2.

(ii) *S. lividans* M715 (Δ*zwf2*). An in-frame deletion mutant for the *zwf2* locus was made by using a strategy similar to that described above for the Δ*zwf1* mutant. The 3′ end of *zwf2* was amplified by PCR by using cosmid StC22 DNA and zwf2bgl2 and zwf2opc2h3 as the primers. The amplified DNA added *Bgl*II and *Hin*dIII sites at the 5′ and 3′ ends, respectively, of the *zwf2* fragment. The DNA fragment was cloned in pGEM-T, and the nucleotide sequence was confirmed by using zwf2.seq6 and the universal and reverse sequencing primers. The DNA fragment was excised with *Bgl*II and *Hin*dIII and ligated with pIJ8706 that had been digested with *Bam*HI and *Hin*dIII. Construction of the in-frame deletion was confirmed by nucleotide sequence analysis by using the universal, reverse, and zwf2.seq2 primers. The deletion construct (pIJ8717) (Fig. 2b) was introduced into *S. lividans* 1326 by conjugation, with selection for apramycin-resistant exconjugants. Purification in the presence of nalidixic acid and apramycin, followed by three rounds of nonselective growth, yielded a population of spores from which apramycin-sensitive colonies were identified at a frequency of ca. 1 in 2,000. PCR analysis of chromosomal DNA derived from the apramycin-sensitive segregants by using zwf2.6 and zwf2.seq2 produced 1.8- and 1.2-kb amplification products for *zwf2*$^+$ strains and *zwf2* deletion mutants, respectively. Two strains were shown to produce the smaller mutant PCR product, and the Δ*zwf2* strains were designated *S. lividans* M715-1 and M715-2, respectively.

(iii) *S. lividans* M706 (Δ*zwf1* Δ*zwf2-opc2-devB*). DNA fragments flanking the 5′ end of *zwf2* and the 3′ end of *devB* were amplified by PCR by using cosmid StC22 DNA. Primers zwf2.1 and zwf2.2 (3′ end of *tal2*) were used to add *Eco*RI and *Bam*HI sites at opposite ends of the fragment containing the 5′ end of *zwf2*. Similarly, primers zwf2.3 and zwf2.4 (3′ end of the gene encoding a hypothetical protein adjacent to and divergent from *devB*) added *Bam*HI and *Hin*dIII sites at the fragment ends. The amplified DNA fragments were cloned into pGEM-T. Nucleotide sequence analysis (performed by using primers zwf2.seq3 and zwf2.seq4, as well as universal and reverse sequencing primers) confirmed that the expected DNA fragment had been isolated for the product of the zwf2.3 and zwf2.4 primers. However, two different PCR errors were observed in DNAs from different colonies (when zwf2.seq1 and zwf2.seq2 as well as universal and reverse

TABLE 2. Oligonucleotides used in this study

Designation	Nucleotide sequence	Cosmid location
g6pdh1	AAAAAAGCTTCCGAGGCCGTCCAGCAGCCACGAG	SC5A7:9,801–9,820
g6pdh2	AGGAGTACTGGGCCTCGCACGACAA	SC5A7:11,535–11,511
g6pdh.seq1	GTTCTCGCCGTCGACCTCGATC	SC5A7:10,151–10,172
g6pdh.seq2	GGTGTCAGACATGGACAGGGGT	SC5A7:10,487–10,508
g6pdh.seq3	TTGTCCGCCTCGGCCTCCACGA	SC5A7:10,801–10,822
g6pdh.seq4	GTTCCGGCCTCGGAGCCGACCC	SC5A7:11,149–11,170
zwf2.1	GAATTCAGTCACGGTCGAAGAGGCCAT	StC22:16,387–16,407
zwf2.2	GGATCCTGACGCCGAAGATGACCAGA	StC22:17,387–17,368
zwf2.3	GGATCCACCACGTACGGAGAACGCCGGGTT	StC22:20,659–20,682
zwf2.4	AAGCTTTACGCGCCCGGCCCGCACCACC	StC22:21,682–21,661
zwf2.seq1	ACCTCTCGCAGATCCACTCCGT	StC22:16,752–16,773
zwf2.seq2	TGTGAAGGACAAGGCGTACAGC	StC22:16,987–17010
zwf2.seq3	ACGAAGGAGCGGTACTTCATGT	StC22:20,919–20,940
zwf2.seq4	GGGCGTCGTCCAGGGAAGCGTA	StC22:21,340–21,361
zwf2.seq6	TCGGTTACCTCGAAGAGGAC	StC22:18,254–18,264
opc2.3	GAATTCATATGGTGCTCACCCTGGTCATCGTCA	StC22:18,910–18,934
opc2.4	GGATCCTCATTTCGCCGCCGCCTTCCTCACC	StC22:19,975–19,851
zwf2bgl2	AGATCTCCATGGCCGAGGACAT	StC22:17,994–18,015
zwf2opc2h3	AAGCTTGATGACGACGAGGGTG	StC22:19,021–19,002
zwf2.6	TTCATGGCCGGCGCCAGCTCCGTCCGT	StC22:18,834–18,798

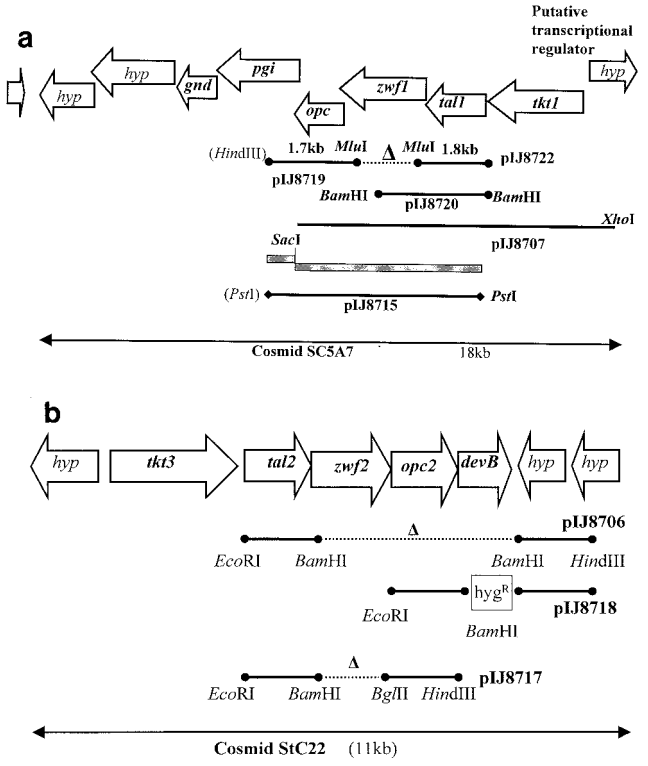

FIG. 2. (a) Map of cosmid SC5A7 containing a cluster of PPP-related genes. The open arrows indicate the directions and extents of the predicted protein-encoding regions. Genes encoding predicted proteins showing strong homology to proteins having known metabolic functions are indicated by boldface italic type. Genes encoding predicted proteins having unknown functions are designated *hyp*. Segments of DNA that were used to make the in-frame *zwf1* deletion are indicated by lines terminating in solid circles. The extent and location of the in-frame deletion in the deletion plasmid pIJ8722 and the Δ*zwf1* deletion strain M704 are indicated by a dotted line. The fragments (from pIJ8707 and pIJ8719) used to produce pIJ8715 are indicated by shaded boxes. The region of the *zwf1* cluster cloned in pIJ8715 and used to complement the Δ*zwf1* mutation is indicated by a line terminating in solid diamonds. Naturally occurring restriction enzyme sites are indicated by boldface type, while sites introduced by PCR or from vector polylinkers are indicated by lightface type in parentheses. (b) Map of cosmid StC22 containing a second cluster of PPP-related genes. The restriction enzyme sites used to join the various fragments were added by using PCR primers. The box labeled hyg^R shows the position of the insertion of the hygromycin resistance gene in the Δ*devB* mutant strain. The extents of deleted DNA in the deletion plasmids and strains are indicated by dotted lines.

primers were used) for the product of amplification with zwf2.1 and zwf2.2. The wild-type sequence of the amplified fragment was obtained by recombining appropriate segments of each clone.

The Δ*zwf2-opc2-devB* deletion plasmid (pIJ8706) was assembled in a three-fragment ligation mixture containing the *Eco*RI-*Bam*HI and *Bam*HI-*Hin*dIII fragments and pKC1132 that had been digested with *Eco*RI and *Hin*dIII. pIJ8706 was introduced into *S. lividans* M704-1 by conjugation. Apramycin-resistant colonies were selected and purified. After three rounds of sporulation on nonselective agar, the progeny were screened for sensitivity to apramycin. Southern hybridization with the cloned *Eco*RI-*Bam*HI fragment containing *tal2* (Fig. 2b) as the probe revealed patterns corresponding to genotypes for either the wild type (a 6.37-kb *Mlu*I fragment) or Δ*zwf2-opc2-devB* (a 5.28-kb *Mlu*I fragment), consistent with loss of the 3.2-kb fragment which included a single *Mlu*I site. Two Δ*zwf2-opc2-devB* colonies were identified (from a population of approximately 4,000 colonies) and were designated M706-1 and M706-2.

(iv) *S. lividans* M714 (Δ*devB*). PCR amplification of cosmid StC22 DNA with the opc2.3 and opc2.4 primers produced a fragment encoding *opc2* with an *Eco*RI site at the 5′ end and a *Bam*HI site at the 3′ end. After cloning and nucleotide sequence confirmation, the fragment was purified and ligated into pIJ8706, which had been digested with the same enzymes. The resulting plasmid was cleaved at its unique *Bam*HI site and treated with calf intestinal alkaline phosphatase before ligation with a *Bgl*II fragment purified from pIJ963 (18), which contained a hygromycin resistance gene. The ligation mixture was used to transform competent cells of *E. coli* DH5α with selection for hygromycin resistance. Digestion of the resulting plasmid (pIJ8718) (Fig. 2b) with *Eco*RI showed that in all of the transformants the hygromycin resistance gene had replaced *devB* and was inserted in the same orientation as the *zwf2* operon. pIJ8718 was introduced into *S. lividans* 1326 by conjugation, which produced strains that were resistant to both hygromycin and apramycin. After nonselective growth, one apramycin-sensitive, hygromycin-resistant colony was isolated after ca. 2,500 colonies were screened. The Δ*devB* strain was designated *S. lividans* M714.

Complementation of Δ*zwf1*. A 768-nucleotide *Hin*dIII-*Sac*I DNA fragment was isolated from pIJ8719 (Fig. 2a), and a 6.52-kb *Sac*I-*Xho*I DNA fragment was isolated from cosmid SC5A7. These two fragments were ligated with pIJ2925 that had been digested with *Hin*dIII and *Sal*I. The resulting plasmid (pIJ8707) contained the majority of the putative *zwf1* operon with the 3′ end truncated within *pgi* (downstream of *opc*) and the 5′ end truncated within a putative divergent transcriptional regulator, the role of which is not known yet (Fig. 2a). A 4.5-kb *Pst*I fragment from pIJ8707 (extending from the polylinker *Pst*I site in pIJ2925 [adjacent to the *Hin*dIII site] to the *Pst*I site at nucleotide 14,308 in SC5A7) was cloned into the *Pst*I site of pKC1132. The resulting plasmid (pIJ8715) contained the 3′ end of *tal1* together with the complete *zwf1* and *opc1* genes and the 5′ end of *pgi*.

pIJ8715 was transferred by conjugation into M704 *(*Δ*zwf1*). Exconjugants were selected with apramycin and nalidixic acid. After purification, colonies were grown nonselectively on SFM agar (three rounds of sporulation) and screened for loss of the apramycin resistance marker. Chromosomal DNA was isolated from candidate strains. Replacement of the in-frame deletion mutant allele by wild-type *zwf1* was confirmed by Southern hybridization by using the 2.8-kb *Bam*HI fragment contained in pIJ8720 as the probe.

Enzyme activity assays. G6PDH (EC 1.1.1.49) assays were based on the production of NADPH, which was measured spectrophotometrically at 340 nm. The conditions used were those described by Lessie and Vander Wyk (19), except that 2-mercaptoethanol was omitted. 6PGDH (EC 1.1.1.43) activity was measured similarly by using either NAD^+ or $NADP^+$. 6-Phosphogluconolactonase was assayed by the method of Collard et al. (11), except that 50 mM Tris-HCl (pH 7.5) was used instead of HEPES (pH 7.1) Protein concentrations were measured by using the Bio-Rad protein assay reagent.

Diamide sensitivity assays. Confluent lawns of strains were generated by pouring 3 ml of soft nutrient agar (containing approximately 10^6 *Streptomyces* spores) onto Difco nutrient agar plates. Paper discs containing 10 μl of either 0.1 or 0.5 M diamide (28) were added, and the plates were photographed after 30 h of incubation at 30°C.

Antibiotic and metabolite estimation. ACT was measured by determining absorbance at 640 nm (molar extinction coefficient value at 640 nm [ε_{640}], 25,320) as described by Bystrykh et al. (7). RED was measured in acidified methanol at 530 nm by using a molar extinction coefficient of 100,500 (17).

Fermentation experiments. The cultivation conditions (in 3-liter Applicon fermentors with a working volume of 1 liter) used for production of ACT in a phosphate-limited minimal medium (containing 10 g of glucose per liter) were the conditions previously described (5) for *S. lividans* 1326/pIJ68. For analysis of RED production in 4-liter Chemap fermentors, 2.5 liters of phosphate-limited Evans minimal medium (13) containing 2 mM NaH_2PO_4 and 25 g of glucose per liter was sterilized for 20 min at 121°C and 500 rpm. The culture was grown at 28°C with stirring at 800 rpm with an aeration rate of 1 volume per volume of liquid per min. pH was controlled between 6.8 and 7.2 by adding 4 M HCl or 4 M NaOH. For estimation of dry cell weight (biomass), 2-ml samples of culture were vacuum filtered through preweighed Whatman GF/C filter paper, washed with 10 ml of distilled water, and dried at 90°C to constant weight. All measurements were done in triplicate. RED production was analyzed by high-performance liquid chromatography. Fermentation broth samples (2 ml) were collected and mixed with an equal amount of acidified methanol. After centrifugation (1,200 × *g* for 10 min) the supernatant was injected for high-performance liquid chromatography analysis with a 5 μm Beckman Ultrasphere octyldecyl silane C_{18} column (4.6 by 250 mm) by using a linear elution gradient ranging from 20% phase B (CH_3OH plus 0.1% trifluoroacetic acid) in phase A (CH_3OH-CH_3CN-H_2O [4:1:5] plus 0.1% trifluoroacetic acid) to 100% phase B in 12 min. The flow rate was 1 ml/min, and the injection volume was 10 μl. The column effluent was monitored at 533 nm. RED was purified and used as an external standard.

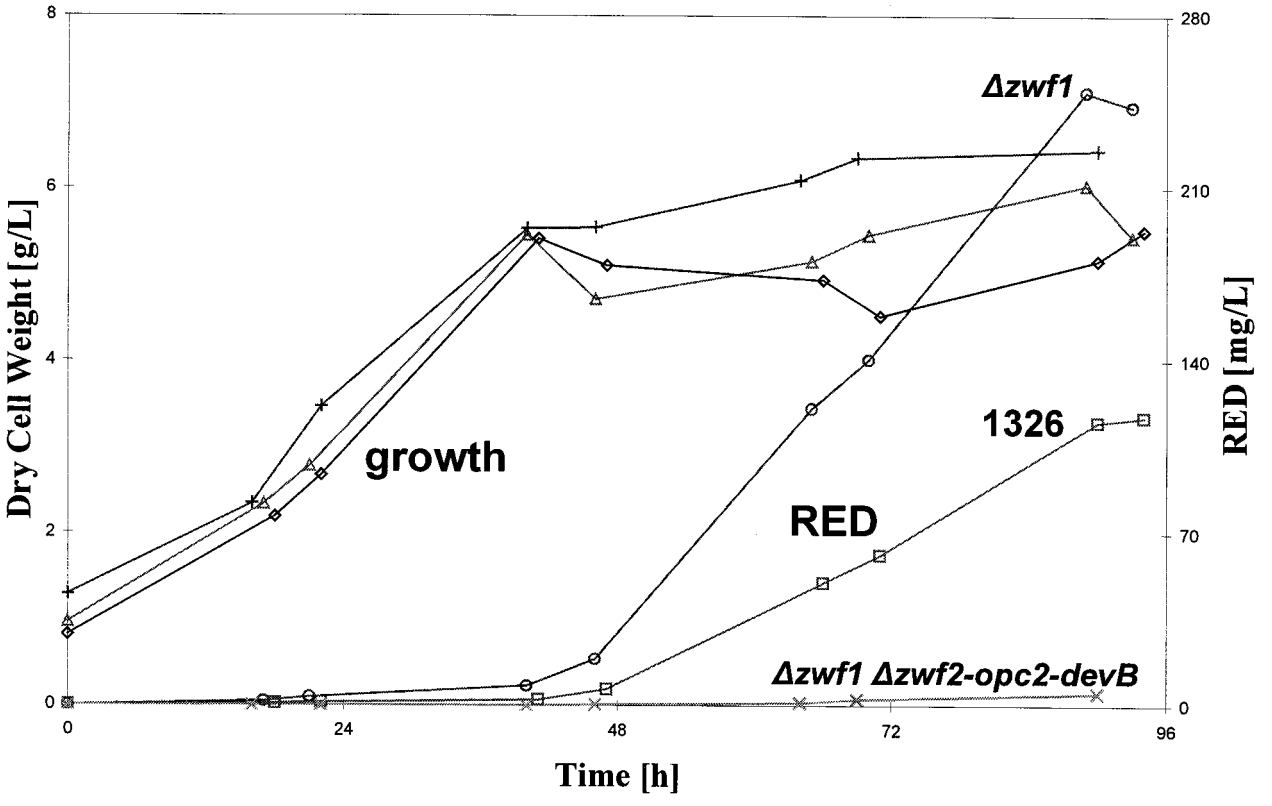

FIG. 3. RED production in fermentors by wild-type and *zwf* mutant *S. lividans* strains carrying multiple copies of the pathway-specific activator gene for RED biosynthesis. Symbols: △, ◇, and +, dry weight of cells of Δ*zwf1* mutant M704, wild-type strain 1326, and Δ*zwf1* Δ*zwf2-opc2-devB* mutant M706, respectively; ○, □, and ×, RED production by *zwf1*, wild-type, and Δ*zwf1* Δ*zwf2-opc2-devB* strains, respectively.

RESULTS

Deletion of *zwf1*. A gene (*zwf1*) encoding a putative G6PDH was identified early in the *S. coelicolor* genome sequencing project in cosmid SC5A7. The putative *zwf1* operon (Fig. 2a) is delineated at one end by a putative transcriptional regulator that is oriented away from the PPP gene cluster. Since *zwf1* appears to lie within a polycistronic transcription unit, an in-frame deletion was made in the gene to eliminate Zwf1 activity without affecting the expression of the downstream genes (*opc*, *pgi*, *gnd*, and two hypothetical genes of unknown function). The resulting strain, M704 (Δ*zwf1*), grew and sporulated normally.

The Zwf and 6PGDH activities present in crude extracts of mycelia of *S. lividans* 1326 and *S. coelicolor* M145 that had been grown for 40 h in YEME were determined. For both strains, specific activities of 9 to 10 nmol min^{-1} mg of $protein^{-1}$ were observed for Zwf, while 6PGDH activity was two- to threefold higher. Enzyme assays with crude extracts of *S. lividans* M704 (Δ*zwf1*) reproducibly produced a specific activity of 4 to 5 nmol min^{-1} mg of $protein^{-1}$ (i.e., a reduction of about 50% compared to wild-type strain 1326). The residual activity was presumed to reflect the presence of another *zwf* gene (see below). The 6PGDH activity in M704 (Δ*zwf1*) was the same as that in the wild-type strain.

Protoplasts of M704 (Δ*zwf1*) were transformed with multicopy plasmids carrying the pathway-specific activator genes for ACT (*act*II-ORF4 on pIJ68) or RED (*redD* on pIJ6014) biosynthesis. For RED production at the 4-liter bioreactor scale, M704/pJ6014 had a maximum volumetric productivity of ca. 250 mg · $liter^{-1}$ after 90 h of fermentation, while control strain 1326/pIJ6014 had a maximum volumetric productivity of about 120 mg · $liter^{-1}$ in the same period (Fig. 3). The growth and production kinetics were similar for the Δ*zwf1* mutant and the control strain, but the mutant produced twice as much RED. The specific productivities were 43 and 22 mg of RED per g (dry weight) of cells, respectively. Similar observations were made for production in shake flask fermentations, with the Δ*zwf1* mutant (M704) showing approximately two- to threefold greater productivity than control strain 1326 (Fig. 4a). The results were expressed in terms of the maximum specific ACT production (in milligrams of ACT per gram [dry weight] of cells). An independently isolated Δ*zwf1* mutant (M704-2) gave the same results. Similarly, shake flask fermentations with M704 Δ*zwf1* and 1326 containing pIJ6014 confirmed the RED fermentation results (Fig. 4b). The Δ*zwf* mutant produced more than twice as much RED as the parental strain. A maximum volumetric productivity of about 180 mg · $liter^{-1}$ was achieved after 90 h of fermentation of M704 (Δ*zwf1*)/pIJ6014, compared with a maximum volumetric productivity of ca. 80 mg · $liter^{-1}$ for 1326/pIJ6014. Lower antibiotic productivity at the shake flask scale than at the bioreactor scale was a constant feature of RED-producing strains during the RapidS Project (Jovetic and Marinelli, unpublished results).

M704 (Δ*zwf1*)/pIJ68 took much longer to start rapid growth

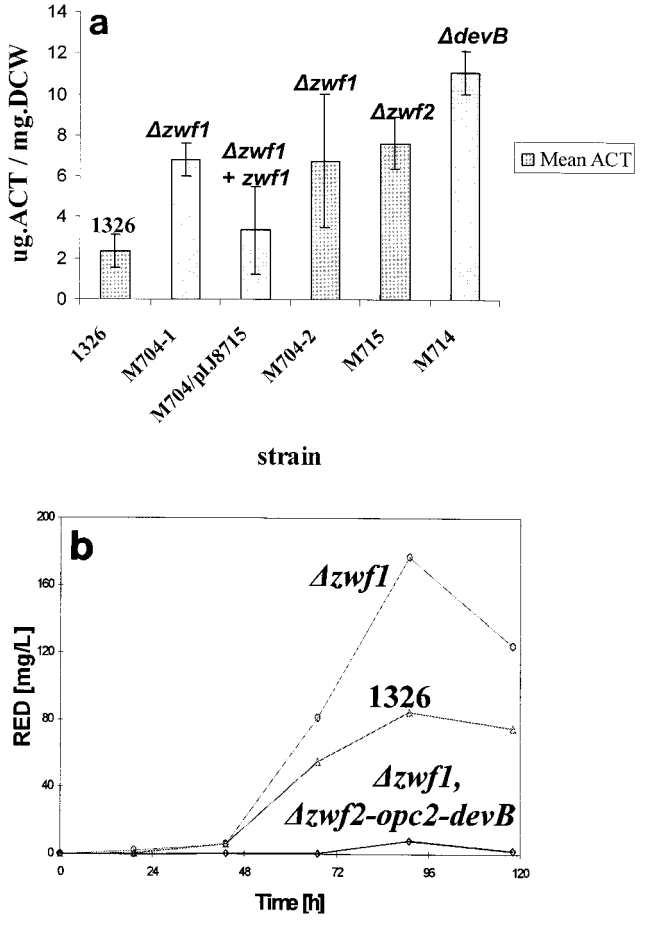

FIG. 4. Antibiotic production in shake flask fermentations with wild-type and mutant *S. lividans* strains. (a) Mean maximum specific ACT production (in micrograms of ACT per milligram [dry weight] of cells [DCW]) for each strain carrying pIJ68. The error bars indicate the standard errors of the means. The strains used and their genetic lesions are indicated. The strain in which Δ*zwf1* was complemented with wild-type DNA was designated M704/pIJ8715. (b) RED production by strains carrying pIJ6014. Symbols: △, wild-type strain; ◇, Δ*zwf1* Δ*zwf2-opc2 devB* strain; and ○, Δ*zwf1* strain.

in 3-liter fermentors than 1326/pIJ68 took (data not shown). However, the specific ACT production (in milligrams of ACT per gram [dry weight] of cells) was substantially higher for the Δ*zwf1* mutant (500 ± 30 mg · g^{-1}) than for the wild-type strain (390 ± 40 mg · g^{-1}) in the stationary phase, in which production reached the highest volumetric rate. In this phase, the yield of ACT (in milligrams of ACT per gram of glucose consumed) was reproducibly 20% higher in M704 (Δ*zwf1*)/pIJ68 cultures than in 1326/pIJ68 cultures (data not shown). Thus, even though ACT production started later in M704 (Δ*zwf1*)/pIJ68, the Δ*zwf1* mutant exhibited better ACT production capability than the parental strain. The growth lag of M704 (Δ*zwf1*)/pIJ68 (which was observed in four different experiments) was not observed with the RED-overproducing strain (Fig. 3) or with the *zwf* double mutant containing pIJ68. No significant differences in growth rates were observed between the strains in shake flask experiments. The reason for the lag in growth of the M704 (Δ*zwf1*)/pIJ68 strain in the fermentors is not clear but may involve the particular inoculum and/or the specific growth conditions used in the ACT fermentor experiments.

Complementation of *S. lividans* M704 (Δ*zwf1*). To verify that the increased production did indeed result from the Δ*zwf1* mutation, the wild-type *zwf1* gene was reintroduced into M704 (Δ*zwf1*) by using a double-crossover strategy that was essentially the reverse of the procedure used to make the in-frame deletion. Protoplasts of the resulting strain were transformed with pIJ68 DNA. Shake flask fermentations (Fig. 4a) showed that the level of ACT production was lower than that in M704 (Δ*zwf1*)/pIJ68 and similar to that in 1326/pIJ68, confirming that the Δ*zwf1* mutation was causally linked to the improvement in ACT production.

Deletion of *zwf2*. The behavior of a Δ*zwf2* mutant was expected to be similar to that of the Δ*zwf1* strain, since the Zwf activity in the latter strain was approximately one-half that in 1326, suggesting that the two Zwf proteins might be equivalent isoforms. Enzyme assays with the Δ*zwf2* mutant, M715, confirmed that it had approximately one-half the Zwf activity of 1326 (data not shown). Shake flask fermentations of M715 (Δ*zwf2*)/pIJ68 showed improved ACT biosynthesis (Fig. 4a), and specific ACT production was essentially equivalent to that observed in M704 (Δ*zwf1*)/pIJ68. This result reinforced the observations made with the Δ*zwf1* mutants and indicated that the changes in antibiotic production reflected changes in the activity of the first step in the PPP.

Δ*zwf1* Δ*zwf2-opc2-devB* mutants. Mutants M706-1 and M706-2 (Fig. 2b) lacking *zwf2* and *devB* together with the intervening gene (*opc2*) were constructed by using the Δ*zwf1* strain (M704). Since the gene having an unknown function that lies downstream of *devB* is oriented in the opposite direction, there should have been no polar effects on the expression of downstream genes. M706-1 and M706-2 (both Δ*zwf1* Δ*zwf2-opc2-devB*) were cultured in YEME for 40 h, and the mycelia were examined for Zwf activity. There was no detectable Zwf activity, whereas 6PGDH activity was present at about the same level as it was in 1326 and M704 (Δ*zwf1*).

The abilities of these strains to generate NADPH were assessed by testing their sensitivities to diamide (which causes the formation of toxic cytoplasmic disulfides in low-molecular-weight thiols and in proteins). In *S. coelicolor*, such oxidative stress is neutralized by thioredoxin reductase, which uses NADPH to reduce the deleterious disulfide bonds (28). When challenged with diamide, M704 (Δ*zwf1*) showed a small but reproducible increase in sensitivity compared to 1326 (Fig. 5). The double *zwf* mutant strains M706-1 and M706-2 (Δ*zwf1* Δ*zwf2-opc2-devB*) showed much larger zones of inhibition, indicating a further increase in sensitivity to diamide.

M706-1 (Δ*zwf1* Δ*zwf2-opc2-devB*) protoplasts were transformed with the transcriptional activator plasmids (pIJ68 and pIJ6014) and with the corresponding vector (pIJ486) as a control. When grown on phosphate-limited Evans medium containing 1.5% agar, the resulting strains appeared to be slightly blue and dark red for the pIJ68 and pIJ6014 derivatives, respectively, indicating that they could still make antibiotic in spite of the double *zwf* deletions. Growth of M706 (Δ*zwf1* Δ*zwf2-opc2-devB*)/pIJ68 in a fermentor resulted in less antibiotic production than growth of either the single Δ*zwf1* mutant (M704) or the wild-type control strain containing the same plasmid. A specific level of ACT production of only 80 ± 9 mg

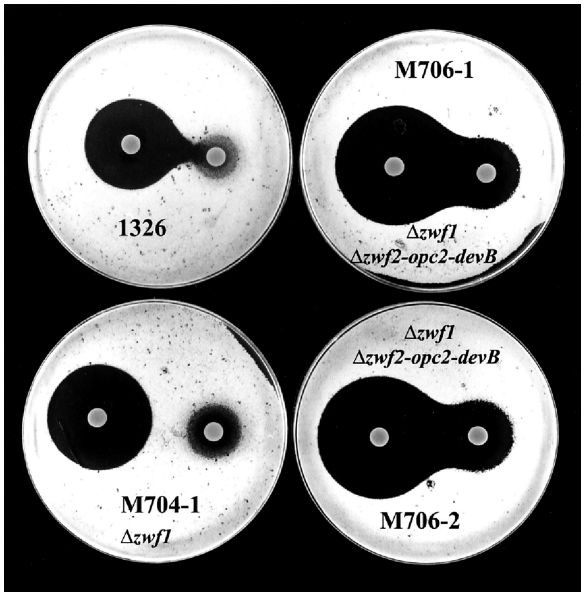

FIG. 5. Increased diamide sensitivity of *S. lividans* mutant strains. The sensitivities of the strains to inhibition of growth by diamide are indicated by zones of clearing (around the diamide-containing discs) on lawns of growth. The larger zones were observed around the discs containing the higher concentrations of diamide (0.5 M compared to 0.1 M).

of ACT per g (dry weight) of cells was observed for the M706 (Δ*zwf1* Δ*zwf2-opc2-devB*) mutant, compared to values of 390 and 500 mg of ACT per g (dry weight) of cells for the wild-type and M704 (Δ*zwf1*) strains, respectively (data not shown). M706 (Δ*zwf1* Δ*zwf2-opc2-devB*)/pIJ68 grew at a rate similar to that of 1326/pIJ68, but ACT production reached a plateau at 140 h and did not increase further, as it did in M704 (Δ*zwf1)*/pIJ68.

Similarly, RED productivity in M706 (Δ*zwf1* Δ*zwf2-opc2-devB*)/pIJ6014 was drastically reduced compared to that in 1326/pIJ6014 and that in M704 (Δ*zwf1*)/pIJ6014 (Fig. 3). The growth patterns of the mutant and control strains were similar for the first 48 h of cultivation. The control strain then started to accumulate RED, whereas M706 (Δ*zwf1* Δ*zwf2-opc2-devB*)/pIJ6014 showed a further increase in biomass but produced only traces of the red pigment. The reduction in antibiotic production was confirmed by shake flask experiments for both ACT (data not shown) and RED (Fig. 4b).

Deletion of *devB*. Since the *zwf* double mutant [M706 (Δ*zwf1*Δ*zwf2-opc2-devB*)] did not produce as much antibiotic as the single-mutant Δ*zwf1* strain (M704), a mutant was made in which only *devB* was inactivated; this mutant was designated M714. A mutation in *devB* might improve antibiotic production capability, since such a strain might show a significantly reduced flux through the PPP without suffering such a large reduction in the ability to produce NADPH.

DevB activity was not detected in the *devB* mutants M714 (Δ*devB*) and M706 (Δ*zwf1* Δ*zwf2-opc2-devB*). In these mutants, the rate of hydrolysis of 6-phosphogluconolactone was indistinguishable from the observed rate of spontaneous hydrolysis (data not shown). In contrast, the Zwf activity of M714 (Δ*devB*) was not significantly different from that of wild-type strain 1326, whereas there was no detectable Zwf activity in M706 (Δ*zwf1* Δ*zwf2-opc2-devB*). The results of these enzyme assays are in complete agreement with the results expected for the mutations. Shake flask fermentation cultures of M714 (Δ*devB*)/pIJ68 had a specific ACT productivity significantly higher than that of any other strain tested in this study (Fig. 4a).

DISCUSSION

We demonstrated that modulation of Zwf activity has a considerable impact on the antibiotic production capability of *S. lividans* strains which were engineered to overproduce ACT or RED. Blocking PPP activity by deleting both *zwf* genes resulted in a marked reduction in antibiotic production. However, when Zwf activity was halved (as in the individual Δ*zwf1* and Δ*zwf2* mutants), antibiotic production increased. The latter observation was surprising, given the positive correlation between methylenomycin production and PPP activity in *S. coelicolor* (26). The results suggest that the production of ACT and RED under the conditions used in these experiments is not limited by the supply of NADPH. Presumably, the NADPH required for growth of the double *zwf* mutant is adequately supplied by tricarboxylic acid cycle activity (e.g., by isocitrate dehdrogenase) and/or transhydrogenase activity (which can reversibly interchange the levels of NADH and NADPH under appropriate conditions). Homologues of genes encoding the two putative transhydrogenase subunits are present in the *S. coelicolor* genome sequence (*pntA* and *pntB*; accession number AL450289), although there has been no biochemical confirmation of their function.

The apparently normal growth characteristics of M706 (Δ*zwf1* Δ*zwf2-opc2-devB*) and its ACT- and RED-overproducing derivatives confirm that the cellular requirements for nucleotide biosynthesis can be adequately met by the reversible transketolase reactions using glycolytic intermediates. While pentose synthesis was unaffected in mammalian cells carrying targeted disruptions of G6PDH (29), the susceptibility of these cells to oxidative stress was markedly enhanced. The increased sensitivity of the *S. lividans zwf* mutants to diamide is indicative of a reduced capacity for NADPH synthesis. However, diamide would also be expected to inactivate the putative PntAB transhydrogenase heterodimer (PntB contains a single cysteine residue). Hence, treatment with this agent may not be representative of the metabolic events occurring during fermentations, in which transhydrogenase activity may augment the supply of NADPH. Less antibiotic was produced by the multiply mutant strain M706 (Δ*zwf1* Δ*zwf2-opc2-devB*) than by the single *zwf* mutants M704 (Δ*zwf1*) and M715 (Δ*zwf2*). This suggests that there is a requirement for some PPP activity (presumably to produce a minimal level of additional NADPH, which cannot be sufficiently supplied by other possible routes) for the production of both ACT and RED. It seems likely that the improvement in antibiotic productivity in the single *zwf* mutants reflects a difference in the rate of carbon flux between the PPP and glycolysis rather than a difference in NADPH production. This interpretation is consistent with the results of chemostat experiments performed with *S. lividans* 1326 containing either pIJ68 or pIJ6014, in which an inverse correlation was noted between the PPP flux and the levels of production of ACT or RED (2). Jonsbu et al. (17) observed a similar relationship between reduced PPP flux and the production of nystatin by

Streptomyces noursei and concluded that the available supply of NADPH was greater than the amount required (41 mmol of NADPH g of nystatin^{-1}). For ACT synthesis, the amount of NADPH required was estimated to be 9.5 mmol g of ACT^{-1} (4). A similar analysis for the RED pathway (Butler, unpublished data) suggested that 30 mmol of NADPH g of RED^{-1} is required (reflecting the highly reduced nature of the acyl side chain). The strains examined in this study produced larger amounts of antibiotic (ACT, ca. 5 to 7 g · liter^{-1}; RED, ca. 240 mg · liter^{-1}) than the nystatin producer (6 to 7 mg · liter^{-1}). However, even at these higher levels the demand for NADPH (66.5, 7.5, and 0.29 mmol · liter^{-1} for ACT, RED, and nystatin, respectively) appears to become limiting only for ACT and RED production in M706 (Δ*zwf1* Δ*zwf2-opc2-devB*). It would be interesting to assess whether the biosynthesis of more reduced macrolides (directed by cloned biosynthetic genes in *S. lividans*) would show a greater dependence on Zwf levels, since these compounds often have a much greater biosynthetic requirement for NADPH. Reduced flux (compared to that in the wild-type strain) through the PPP would lower the loss of carbon (as CO_2), which might lead to higher levels of the glycolytic intermediates required for the production of malonyl coenzyme A, ATP, and potentially other intermediates required for antibiotic production. Hence, providing that the appropriate NADPH availability is achieved, this effect of improved antibiotic production may be generally applicable.

The *S. coelicolor* genome also contains a gene whose product is homologous to a flavin-dependent G6PDH. This activity has been observed in mycobacteria and *Nocardia* spp. (32) and has been shown to use a flavin cofactor (F420) rather than NADPH. Purwantini et al. detected no activity in *S. lividans*, so it is unlikely that this flavin-dependent enzyme contributes to carbon flux through the PPP. The activity was assayed by using the F420 purified from *Mycobacterium thermoautotrophicum*, and it is formally possible that a structurally different cofactor might be required for the *Streptomyces* enzyme.

The improvement in ACT productivity observed in the *devB* mutant (M714) also suggests that it is changes in flux through the PPP that are largely responsible for the effects on antibiotic production observed here. Loss of the activity of DevB is likely to have much more impact on flux through the PPP than mutations in any one of the *zwf* genes have, because DevB is the only protein known to be catalytically involved in hydrolysis of 6-phosphogluconolactone (23). The results also suggest that there are no significant adverse effects produced by potential accumulation of the toxic compound 6-phosphogluconolactone (33) in the organism under the conditions examined. Although the lactone can undergo spontaneous hydrolysis, the low rate of this reaction would still be likely to cause a significant reduction in flux through the PPP. NADPH production by the Zwf activities may be affected (either directly or indirectly) by the accumulation of 6-phosphogluconolactone. Therefore, it is not yet possible to attribute the improvement in antibiotic production solely to a reduction in carbon flux through the PPP rather than to a reduction in the available NADPH concentration. It would be interesting to probe these interpretations experimentally by performing a metabolic flux analysis of strains in which PPP activity is inducibly expressed (39) and to examine the effects of induction on antibiotic production at a variety of times during fermentation. Overexpression of the *zwf* genes appears to require coexpression of the adjacently located (presumably cotranscribed) *opc* gene. In contrast to the successful production of human G6PDH (1) for crystallography, attempts to overproduce both the Zwf proteins of *S. coelicolor* in *E. coli* produced soluble but inactive protein (Butler, unpublished). This implies that the streptomycete Zwf proteins are assembled into heteromeric active proteins with their corresponding Opc proteins. This biochemical organization occurs in *C. glutamicum* (25), and the OpcA protein in *Nostoc punctiforme* ATCC 29133 (15) appears to play a role as an allosteric activator of the Zwf protein. In contrast, the 6-phosphogluconolactonase was expressed as a soluble, active protein in *E. coli* (Butler, unpublished), suggesting that no cofactors specific for the *Streptomyces* enzyme are necessary for this enzymatic activity.

While the results of Obanye et al. (26) suggest that methylenomycin production should be reduced in the mutants described here, the effect on the synthesis of more highly reduced compounds remains to be determined. Other metabolic approaches have also been used to enhance secondary metabolite production in actinomycetes (9, 20, 24, 31). The mutations and strains described here add to the available repertoire of tools that can be used to increase the yields of a potentially wide range of secondary metabolites.

ACKNOWLEDGMENTS

This work was supported by EU Cell Factory grant B104-CT96-0332 to Mervyn Bibb (coordinated by R. Luiten) and BBSRC grant 208/P14580.

We are grateful to K. F. Chater, D. A. Hopwood, M. Elliot, and G. Sawers for comments on the manuscript. M. J. Buttner, T. Palmer, S. Rawsthorne, and A. Smith are thanked for helpful discussions. We thank P. Jakimowicz, T. Kieser, and E. Takano for help with preparation of figures. We also thank J. K. M. Brown for help with statistical analysis (using the Genstat software) and S. Riches for help with preparation of the manuscript.

REFERENCES

1. **Au, S. W. N., C. E. Naylor, S. Gover, L. Vandeputte-Rutten, D. A. Scopes, P. J. Mason, L. Luzzatto, V. M. S. Lam, and M. J. Adams.** 1999. Solution of the structure of tetrameric human glucose-6-phosphate dehydrogenase by molecular replacement. Biol. Crystallogr. D **55:**826–834.
2. **Avignone-Rossa, C., J. White, A. Kuiper, P. W. Postma, M. J. Bibb, and M. J. Texeira de Mattos.** 2002. Carbon flux distribution in chemostat cultures of *Streptomyces lividans.* Metab. Eng. **4:**138–150.
3. **Bierman, M., R. Logan, K. O'Brien, E. T. Seno, R. Nagaraj Rao, and B. Schoner.** 1992. Plasmid cloning vectors for the conjugal transfer of DNA from *Escherichia coli* to *Streptomyces* spp. Gene **116:**43–49.
4. **Bruheim, P., M. J. Butler, and T. E. Ellingsen.** 2002. A theoretical analysis of the biosynthesis of actinorhodin in a hyper-producing *Streptomyces lividans* strain cultivated on various carbon sources. Appl. Microbiol. Biotechnol. **58:**735–742.
5. **Bruheim, P., H. Sletta, M. J. Bibb, J. White, and D. W. Levine.** 2002. High yield actinorhodin production in fed-batch culture by a *Streptomyces lividans* strain over-expressing the pathway-specific activator gene *act*II-ORF4. J. Ind. Microbiol. Biotechnol. **28:**103–111.
6. **Butler, M. J., J. Deutscher, P. W. Postma, T. J. G. Wilson, A. Galinier, and M. J. Bibb.** 1999. Analysis of a *ptsH* homologue from *Streptomyces coelicolor* A3(2). FEMS Microbiol. Lett. **177:**279–288.
7. **Bystrykh, L. V., M. A. Fernandez-Moreno, J. K. Herrema, F. M. Malpartida, D. A. Hopwood, and L. Dijkhuizen.** 1996. Production of actinorhodin-related "blue pigments" by *Streptomyces coelicolor* A3(2). J. Bacteriol. **178:**2238–2244.
8. **Chater, K. F.** 1990. The improving prospects for yield increase by genetic engineering in antibiotic-producing streptomycetes. Bio/Technology **8:**115–121.
9. **Chen, G., G.-Y. Wang, X. Li, B. Waters, and J. E. Davies.** 2000. Enhanced production of microbial metabolites in the presence of dimethyl sulfoxide. J. Antibiot. **53:**1145–1153.
10. **Cole, S. T., R. Brosch, J. Parkhill, T. Garnier, C. Churcher, D. Harris, S. V.**

Gordon, K. Eiglmeier, S. Gas, C. E. Barry III, F. Tekaia, K. Badcock, D. Basham, D. Brown, T. Chillingworth, R. Connor, R. Davies, K. Devlin, T. Feltwell, S. Gentles, N. Hamlin, S. Holroyd, T. Hornsby, K. Jagels, A. Krogh, J. McLean, S. Moule, L. Murphy, K. Oliver, J. Osborne, M. A. Quail, M.-A. Rajandream, J. Rogers, S. Rutter, K. Seeger, J. Skelton, R. Squares, S. Squares, J. E. Sulston, K. Taylor, S. Whitehead, and B. G. Barrell. 1998. Deciphering the biology of *Mycobacterium tuberculosis* from the complete genome sequence. Nature **393:**537–543.

11. **Collard, F., J.-F. Collet, I. Gerin, M. Veiga-da-Cunha, and E. Van Schaftingen.** 1999. Identification of the cDNA encoding human 6-phosphogluconolactonase, the enzyme catalyzing the second step of the pentose phosphate pathway. FEBS Lett. **459:**223–226.
12. **Dekleva, M. L., and W. R. Strohl.** 1988. Biosynthesis of ε-rhodomycinone from glucose by *Streptomyces* C5 and comparison with intermediary metabolism of other polyketide-producing streptomycetes. Can. J. Microbiol. **34:** 1235–1240.
13. **Evans, C. G. T., D. Herbet, and D. W. Tempest.** 1970. The continuous culture of microorganisms. 2. Construction of a chemostat. Methods Microbiol. **2:**277–327.
14. **Hagen, K. D., and J. C. Meeks.** 2001. The unique cyanobacterial protein OpcA is an allosteric effector of glucose-6-phosphate dehydrogenase in *Nostoc punctiforme* ATCC29133. J. Biol. Chem. **276:**11477–11486.
15. **Hager, P. W., H. W. Calfee, and P. V. Phibbs.** 2000. The *Pseudomonas aeruginosa devB/SOL* homolog, *pgl*, is a member of the *hex* regulon and encodes 6-phosphogluconolactonase. J. Bacteriol. **182:**3934–3941.
16. **Hopwood, D. A.** 1997. Genetic contributions to understanding polyketide synthases. Chem. Rev. **97:**2465–2498.
17. **Jonsbu, E., B. Christiensen, and J. Nielsen.** 2001. Changes of in vivo fluxes through central metabolic pathways during the production of nystatin by *Streptomyces noursei* in batch culture. Appl. Microbiol. Biotechnol. **56:**93–100.
18. **Kieser, T., M. J. Bibb, M. J. Buttner, K. F. Chater, and D. A. Hopwood.** 2000. Practical *Streptomyces* genetics. John Innes Foundation, Norwich, United Kingdom.
19. **Lessie, T. G., and J. C. Vander Wyk.** 1972. Multiple forms of *Pseudomomas multivorans* glucose-6-phosphate and 6-phosphogluconate dehydrogenases: differences in size, pyridine nucleotide specificity and susceptibility to inhibition by adenosine 5′-triphosphate. J. Bacteriol. **110:**1107–1117.
20. **Lombo, F., B. Pfeifer, T. Leaf, S. Ou, Y. S. Kim, D. E. Cane, P. Licari, and C. H. Khosla.** 2001. Enhancing the atom economy of polyketide biosynthetic processes through metabolic engineering. Biotechnol. Prog. **17:**612–617.
21. **MacNeil, D. J., K. M. Gewain, C. L. Ruby, G. Dezeny, P. Gibbons, and T. MacNeil.** 1992. Analysis of *Streptomyces avermitilis* genes required for avermectin biosynthesis utilising a novel integration vector. Gene **111:**61–68.
22. **Mahr, K., G. P. van Wezel, C. Svensson, U. Krengel, M. J. Bibb, and F. Titgemeyer.** 2000. Glucose kinase of *Streptomyces coelicolor* A3(2): large-scale purification and biochemical analysis. Antonie Leeuwenhoek **78:**253–261.
23. **Miclet, E., V. Stoven, P. A. Michels, F. R. Opperdoes, J.-M. Lallemand, and F. Duffieux.** 2001. NMR spectroscopic analysis of the first two steps of the pentose-phosphate pathway elucidates the role of 6-phosphogluconolactonase. J. Biol. Chem. **276:**34840–34846.
24. **Minas, W., P. Brunker, P. T. Kallio, and J. E. Bailey.** 1998. Improved erythromycin production in a genetically engineered industrial strain of *Saccharopolyspora erythraea*. Biotechnol. Prog. **14:**561–566.
25. **Moritz, B., K. Striegel, A. A. De Graaf, and H. Sahm.** 2000. Kinetic properties of the glucose-6-phosphate and 6-phosphogluconate dehydrogenases from *Corynebacterium glutamicum* and their applications for predicting pentose phosphate pathway flux. Eur. J. Biochem. **267:**3442–3452.
26. **Obanye, A. I. C., G. Hobbs, D. C. J. Gardner, and S. G. Oliver.** 1996. Correlation between carbon flux through the pentose phosphate pathway and production of the antibiotic methylenomycin in *Streptomyces coelicolor* A3(2). Microbiology **142:**133–137.
27. **Paget, M. S. B., L. Chamberlin, A. Atrih, S. J. Foster, and M. J. Buttner.** 1999. Evidence that the extracytoplasmic function sigma factor σ^E is required for normal cell wall structure in *Streptomyces coelicolor* A3(2). J. Bacteriol. **181:**204–211.
28. **Paget, M. S. B., J.-G. Kang, J.-H. Roe, and M. J. Buttner.** 1998. σR, an RNA polymerase sigma factor that modulates expression of the thioredoxin system in response to oxidative stress in *Streptomyces coelicolor* A3(2). EMBO J. **17:**5776–5782.
29. **Pandolfi, P. P., F. Sonati, R. Rivi, P. Mason, F. Grosveld, and L. Luzzatto.** 1995. Targeted disruption of the housekeeping gene encoding glucose-6-phosphate dehydrogenase (G6PD): G6PD is dispensible for pentose synthesis but essential for defense against oxidative stress. EMBO J. **14:**5209–5215.
30. **Passantino, R., A.-M. Puglia, and K. F. Chater.** 1991. Additional copies of the *actII* regulatory gene induce actinorhodin production in pleiotropic *bld* mutants of *Streptomyces coelicolor* A3(2). J. Gen. Microbiol. **137:**2059–2064.
31. **Pfeifer, B. A., S. J. Admiraal, H. Gramajo, D. E. Cane, and C. H. Khosla.** 2001. Biosynthesis of complex polyketides in a metabolically engineered strain of *E. coli*. Science **291:**1790–1792.
32. **Purwantini, E., T. Gillis, and L. Daniels.** 1997. Presence of F420-dependent glucose-6-phosphate dehydrogenase in *Mycobacterium* and *Nocardia* species, but absence in *Streptomyces* and *Corynebacterium* species and methanogenic Archaea. FEMS Microbiol. Lett. **146:**129–134.
33. **Rakitzis, E. T., and P. Papandreou.** 1998. Reactivity of 6-phosphogluconolactone with hydroxylamine: the possible involvement of glucose-6-phosphate dehydrogenase in endogenous glycation reactions. Chem.-Biol. Interact. **113:**205–216.
34. **Salas, J. A., L. M. Quiros, and C. Hardisson.** 1984. Pathways of glucose catabolism during germination of *Streptomyces* spores. FEMS Microbiol. Lett. **22:**229–233.
35. **Sambrook, J., E. F. Fritsch, and T. Maniatis.** 1989. Molecular cloning: a laboratory manual, 2nd ed. Cold Spring Harbor Press, Cold Spring Harbor, N.Y.
36. **Stryer, L.** 1995. Biochemistry, 4th ed. W. H. Freeman and Company, New York, N.Y.
37. **Sundaram, S., H. Karakaya, D. J. Scanlan, and N. H. Mann.** 1998. Multiple oligomeric forms of glucose-6-phosphate dehydrogenase in cyanobacteria and the role of OpcA in the assembly process. Microbiology **144:**1549–1556.
38. **Takano, E., H. C. Gramajo, E. Strauch, N. Andres, J. White, and M. J. Bibb.** 1992. Transcriptional regulation of the *redD* transcriptional activator gene accounts for growth-phase-dependent production of the antibiotic undecylprodigiosin in *Streptomyces coelicolor* A3(2). Mol. Microbiol. **6:**2797–2804.
39. **Takano, E., J. White, C. J. Thompson, and M. J. Bibb.** 1995. Construction of thiostrepton-inducible, high-copy-number expression vectors for use in *Streptomyces* spp. Gene **166:**133–137.